

Mitigation of cogging torque in surface permanent magnet brushless DC motor using slot opening shift

Introduction. Cogging torque deteriorates the torque quality of surface permanent magnet brushless DC (PMBLDC) motors. **Problem.** Reducing cogging torque is indispensable for performance upgradation of PMBLDC motors; hence, it is an important issue for motor designers. **Goal.** This paper presents a slot opening shift approach to reduce the cogging torque of radial flux surface PMBLDC motors. **Methodology.** A 200 W, 1000 rpm radial flux surface PMBLDC motor is first designed based on different assumed design variables and is treated as a reference model. The parallel stator teeth are uniformly distributed along the stator periphery, and the slot opening is considered in the middle position in the reference design. The cogging torque of the reference design is obtained from simulation and electromagnetic analysis. **Results.** A series of finite element simulations are performed to examine the impact of design upgradation on the cogging torque of the surface PMBLDC motor. It is observed that the peak-to-peak cogging torque is reduced by 44.5 %. **Scientific novelty.** The design is enhanced by applying slot opening shift to stator slots. The slot opening is shifted in an anticlockwise direction, and subsequently, the cogging torque waveform is determined for the upgraded motor from finite element modelling and analysis. **Practical value.** Research has revealed that this technique is effective in reducing cogging torque, and it can also be applied to other topologies of permanent magnet motors. References 23, tables 2, figures 12. **Key words:** brushless motor, finite element analysis, slot opening shift, cogging torque.

Вступ. Пульсація крутного моменту погіршує його якість у безщіткових двигунах постійного струму з постійними магнітами (PMBLDC). **Проблема.** Зниження пульсації крутного моменту є необхідною умовою підвищення продуктивності PMBLDC двигунів, тому це є важливим завданням для проєктувальників двигунів. **Мета.** У статті представлений підхід, заснований на зміщенні пазів для зниження пульсації крутного моменту PMBLDC двигунів з радіальними поверхневими магнітними потоками. **Методологія.** Спочатку проєктується PMBLDC двигун з радіальними поверхневими магнітними потоками потужністю 200 Вт та частотою обертання 1000 об/хв на основі різних передбачуваних проєктних змінних, що розглядається як еталонна модель. Паралельні зубці статора рівномірно розподілені по периферії статора, а паз еталонної конструкції розташований посередині. Пульсація крутного моменту еталонної конструкції отримана з моделювання та електромагнітного аналізу. **Результати.** Проведено ряд скінченно-елементних моделювань для вивчення впливу вдосконаленої конструкції на пульсацію крутного моменту PMBLDC двигуна з поверхневими магнітами. Встановлено, що пікова пульсація крутного моменту знижується на 44,5 %. **Наукова новизна.** Конструкція вдосконалена за рахунок застосування усунення відкриття пазів статора. Відкриття паза зміщується проти годинникової стрілки, і згодом форма пульсації моменту модернізованого двигуна визначається за допомогою скінченно-елементного моделювання та аналізу. **Практична значимість.** Дослідження показали, що цей метод є ефективним для зниження пульсації крутного моменту, і його також можна застосовувати до інших топологій двигунів з постійними магнітами. Бібл. 23, табл. 2, рис. 12.

Ключові слова: безщітковий двигун, аналіз методом скінченних елементів, зсув відкриття пази, крутний момент зубчатого обертання.

Introduction. Brushless DC motors offer better operational efficiency, a high power-to-volume ratio, a varied speed range, and rapid dynamic response. Due to these characteristics, it has gained widespread acceptance in various residential and industrial applications. Progress in material technology in permanent magnet (PM) and semiconductor switches has accelerated the development of brushless DC motors. Apparent torque ripple is one of the biggest problems in permanent magnet brushless DC (PMBLDC) motors. Torque ripple produces vibration and unwanted audible noise which may deteriorate the overall performance of the motor. The development of smooth torque in brushless DC motors is a prime objective that needs thorough attention to all aspects of motor design. Torque ripple is inherent in brushless DC motors due to cogging torque (CT), distorted back electromotive force (EMF) waveform, non-ideal exciting current waveform, and time delay in excitation pattern [1–3]. The torque ripple of brushless DC motors can be reduced by either decreasing the CT or improving the quality of back EMF and exciting current waveforms. Reducing CT is a design issue, while improving the quality of back EMF and exciting current waveforms is a control issue. Any variation in control techniques results in reduced operational efficiency of brushless DC motor drives. CT is the major cause in brushless DC motors for producing torque ripple. CT is inherent because of the existence of PMs and a slotted stator structure. The combination of the number of rotor poles and the number of stator slots significantly affects the torque quality and output of the PMBLDC motor. Inappropriate combination of number of rotor poles and stator slots results in a high CT and torque ripple [4]. The CT of PM motors

cannot be eliminated, but can be decreased with design improvements. The reduction of torque ripple is indispensable for applications that require smooth running. Ideally, the torque ripple reduction technique should only improve torque quality without affecting other performance parameters of the motor. The average CT value is zero, and its variation is achieved by unexcited stator windings. CT is large for a more compact motor, having a smaller air gap and stronger PM. CT reduction is a significant concern while designing the PMBLDC motor and is considered an important criterion for the quality of motor design. Reduction of CT is a difficult task and it cannot be eliminated but can be reduced to a certain extent [5].

In literature different techniques are available to decrease the CT from a design perspective. Skewing, shaping of PM, displacing magnets, inclusion of dummy slots, variation of magnet pole arc, dual notching, slot displacement and use of fractional number of slots are a few methods used to mitigate CT of PM motors [6–21]. The length of the stator conductor and hence copper losses increase with the application of skewing of the stator slot. One of the most popular approaches for mitigating CT is the skewing of PM. However, the stray losses and leakage inductance increase, and the useful magnetic flux linking with the stator winding decreases. It also produces unbalanced axial electromagnetic force which produces vibration and acoustic noise besides damaging the bearing system. Shaping of PM reduces CT but it adversely affects the back EMF waveform. Displacing magnets and rotors cause the rotor's center of mass to shift away from the rotating axis. The use of

dummy slots or teeth reduces the amplitude and increases the frequency of CT. But an important drawback of this method is manufacturing difficulties which results in increased cost of motor. In the fractional number of slots, each magnet has a different placement compared to stator slots. Therefore, CT components due to individual PM poles are out of phase relative to each other. Hence, the resulting CT is decreased due to the mutual cancellation of the sub-components of CT.

Goal. This paper presents a slot opening shift approach to reduce the cogging torque of radial flux surface PMBLDC motors.

Cogging torque. The slot opening shift method's influence on surface PMBLDC motor performance is examined and presented. Extensive simulations utilizing finite element (FE) modelling and analysis [22] are conducted to arrive at a result. CT and its associated equations are explained. A detailed explanation of the reference PMBLDC motor model is provided. An enhanced design is introduced that utilizes a slot opening shift mechanism to reduce the CT of the reference BLDC motor.

CT is immanent in PM motors due to the association between air-gap permeability changes and rotor magnetomotive force. CT exists without stator current and is periodic in nature. The subsequent equation represents the CT generated in PMBLDC motors in the absence of skewing [23]:

$$T_{cog} = \sum_{k=1}^{\infty} T_{N_{pk}} \sin(N_{pk}\alpha), \quad (1)$$

where k is the order of harmonics; N_p is the number of CT cycles in one mechanical rotation; it is determined by LCM of the number of stator slots (N_s), and the number of rotor poles (p); α is the angular difference between the stator's and the rotor's teeth; $T_{N_{pk}}$ is the coefficient resulting from the fast Fourier transform (FFT) of the CT profile.

Equation (1) is used for each stator tooth of the motor to calculate the total CT. The total CT is the cumulative effect of the CTs produced by each stator tooth. The N_{pk} in (1) must be a multiple of the rotor pole numbers p . The CT produced can be shown as the ratio of N_{pk} to p , denoted by i , for any given teeth represented by j (where $1 \leq j \leq N_s$):

$$T_{scj} = \sum_{i=1}^{\infty} T_{sci} \sin pi(\alpha + \phi_j), \quad (2)$$

where T_{sci} is the Fourier coefficient; ϕ_j is the positioning of tooth number j of the stator, with respect to tooth number 1 of the reference stator.

Hence,

$$\phi_j = 2\pi(j-1)/N_s.$$

By adding together, the CT contributions from each of the N_s stator teeth, the total CT can be calculated as:

$$T_{cog} = \sum_{j=1}^{N_s} \sum_{i=1}^{\infty} T_{sci} \sin pi \left(\alpha + \frac{2\pi}{N_s}(j-1) \right). \quad (3)$$

From (3), when p/N_s is a whole number, then regardless of teeth number j :

$$\sin pi \left(\alpha + \frac{2\pi}{N_s}(j-1) \right) = \sin pi\alpha.$$

This indicates that the CT produced by each stator tooth and the total CT are in phase with each other. Therefore, the total CT is equal to the product of N_s and individual CT, and can be represented as:

$$T_{cog} = N_s \sum_{i=1}^{\infty} T_{sci} \sin pi\alpha. \quad (4)$$

The CT produced by dissimilar tooth is out of phase if the ratio p/N_s is not a whole number. Consequently, equation (3) poses a challenge in terms of simplification. A set of a specific number of adjacent slots can be arranged to find the solution. The groups are selected such that the CT generated by different groups is always in phase. As a result, there is a direct correlation among the total CT and the CT of each group [23].

Taking into account λ neighbouring slots (tooth) as a single group, $\lambda = N_p/p$. Using the formula $n = N_p/N_s$, the number of groups (n), can be calculated. The CT for a specific tooth j is represented by (2), which can be reformulated as:

$$T_{scj} = \sum_{i=1}^{\infty} T_{sci} \sin pi \left[\alpha + \frac{2\pi}{N_s}(j-1) \right]. \quad (5)$$

The CT produced by a specific group of λ teeth is determined by adding up the CTs created by individual tooth within this group. This can be expressed as:

$$T_{cog} = \sum_{j=1}^{\lambda} \sum_{i=1}^{\infty} T_{sci} \sin \left[pi \left(\alpha + \frac{2\pi}{N_s}(j-1) \right) \right]. \quad (6)$$

Equation (6) can be simplified as:

$$T_{cog} = \sum_{i=1}^{\infty} T_{sci} \frac{\sin(p\lambda\pi/N_s)}{\sin(p\pi/N_s)} \sin \left[pi\alpha + \frac{p\lambda\pi}{N_s} - \frac{p\pi}{N_s} \right]. \quad (7)$$

Since $p\lambda i/N_s$ in (7) is an integer number, value of $\sin(p\lambda\pi/N_s)$ is zero. Therefore, just the CT component will be present for a specific harmonic index i . Equation (7) can be shortened to these values of i and is expressed as:

$$T_{cog} = \sum_{i=1}^{\infty} T_{sci} \lambda \sin pi\alpha. \quad (8)$$

To get total CT, multiply the CT of a single group, as provided by (8), by the number of groups n :

$$T_{cog} = n \sum_{i=1}^{\infty} T_{sci} \lambda \sin pi\alpha. \quad (9)$$

Design of reference motor. The first motor designed for the analysis is a 200 W, 1000 rpm surface mounted PMBLDC motor, which serves as a reference motor. Figure 1 displays the reference motor's cross-sectional view.

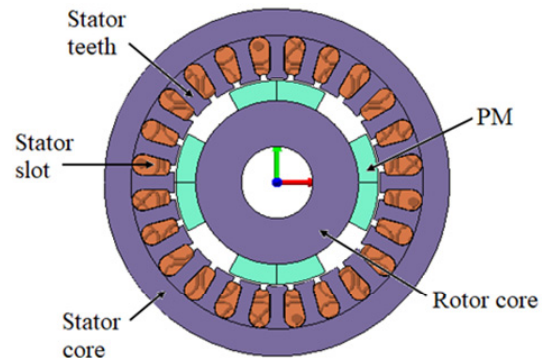


Fig. 1. Reference radial flux PMBLDC motor

The motor is designed by selecting suitable values of various design variables viz., specific magnetic and electric loadings, slot fill factor, distribution factor and pitch factor of winding, stacking factor of laminations, conductor current density etc. The FE model of the reference PMBLDC motor is created in accordance with the design calculations, and appropriate materials are assigned in respective sections. The neodymium iron-

boron (NdFeB) material is used as PM material for better performance. PMs are fixed on the periphery of the rotor. NdFeB holds the maximum energy product of all commercially available magnets at room temperature. High flux density in air gap due to the application of NdFeB leads to remarkable reductions in motor frame size for the same rating. The laminations of stator and rotor are allocated M19 silicon steel material. The specific iron loss of M19 silicon steel material at 1.4 T and 50 Hz frequency is 2 W/kg. The design particulars of the reference BLDC motor are given in Table 1.

Table 1

Design details of reference BLDC motor	
Stator's outer diameter, mm	87
Rotor's outer diameter, mm	51
Stack length, mm	50
Stator's inner diameter, mm	52
Width of stator teeth, mm	3.5
Slot opening, mm	1.7
Magnet pole arc, degree	57
Number of slots	24
Number of phases/poles	3/4
Magnet's thickness, mm	5
Air gap length, mm	0.5
Type of PM	NdFeB
Stator and rotor core material	M19, 29 Ga

The FE model of reference surface mounted BLDC motor is devised using commercially available FE software and an appropriate boundary condition is assigned. The solver creates meshing and the model is divided into triangular elements [22]. Several simulation exercises were performed to acquire the CT waveform of reference motor. With the stator winding unenergized, the rotor is mechanically rotated by 1° increments up to 15°. The torque value obtained for each degree of rotation of the rotor is noted and the curve is plotted between torque values and rotor positions.

It has been analyzed that the reference PMBLDC motor has a peak-to-peak CT of 1.1 N-m. The CT profile is shown in Fig. 2.

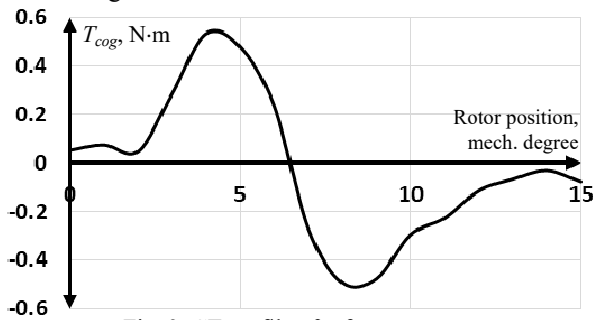


Fig. 2. CT profile of reference motor

The average torque output of the motor is calculated using 2D FE analysis. The rotor is created as a motion component in this analysis, and rotated at the rated speed of 1000 rpm. The correct operation of the inverter energizes stator winding. The torque at distinct rotor positions is calculated and shown against them. Figure 3 depicts the torque waveform of the reference motor. The average torque derived from FE analysis is 1.91 N-m.

Upgraded design using slot-opening shift approach. The CT profile is periodic because of the symmetrical structure of PM motors. The magnitude of harmonics of CT should be reduced to mitigate vibration. Conventional skew of slots and slot openings result in to decentralization of winding function and deterioration of

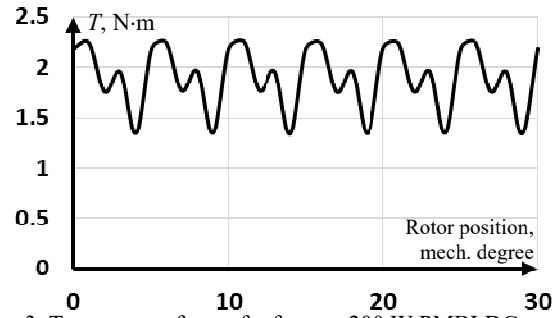


Fig. 3. Torque waveform of reference 200 W PMBLDC motor

back EMF waveform. The air-gap reluctance variation is due to slot openings hence shifting of only slot openings smooths the air-gap reluctance variation without adversely affecting back EMF waveform. This can be considered as an apparent advantage of slot opening shifting in comparison to slot skewing. Slot openings are in the middle in the reference design of the 200 W PMBLDC motor. The upgraded design accomplishes the slot openings shifted in an anticlockwise direction by 3.75° mechanical. Stator stampings of reference design and upgraded design are illustrated respectively in Fig. 4.

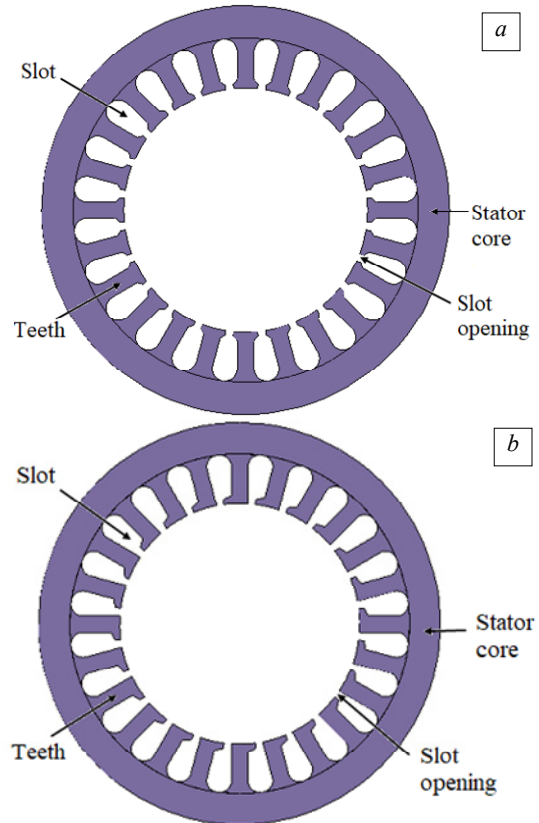


Fig. 4. Stator stampings: a – reference design; b – upgraded design

An upgraded model with shifted stator slot openings in an anticlockwise direction is shown in Fig. 5. All other design details of the upgraded model are the same as the reference model.

Figure 6 depicts a comparison of the reference and modified motors' CT patterns. It is analyzed that the reference design has a CT (peak-to-peak) of 1.1 N-m. When the slot opening of all slots is shifted in an anticlockwise direction, the CT (peak-to-peak) obtained is 0.61 N-m. The CT (peak-to-peak) decreases from 1.1 N-m to 0.61 N-m as slot openings shift anticlockwise.

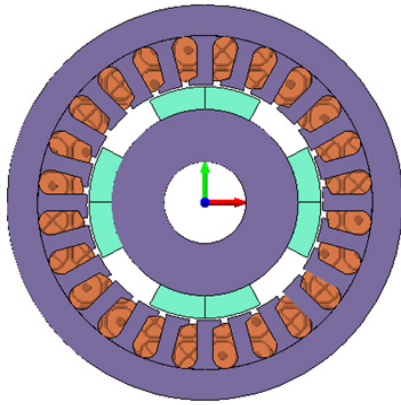


Fig. 5. Radial flux PMBLDC motor with the shifted slot opening

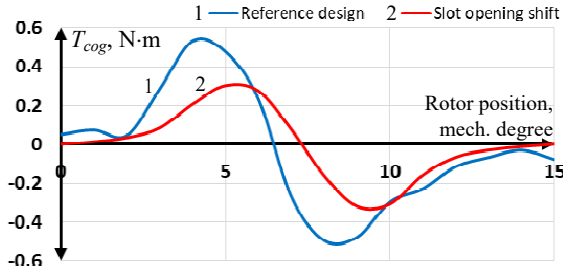


Fig. 6. Comparison of CT profiles

Table 2 depicts variation in CT with slot-opening shift methods. Slot openings are shifted in the anticlockwise direction. It is observed that a 44.5 % reduction in CT (peak-to-peak) is attained with a borderline drop in average torque.

Table 2

Comparison between reference and upgraded design

Design details	CT (peak-to-peak), N-m	Average torque, N-m
Reference design	1.1	1.91
Upgraded design with slot-opening shift in the anticlockwise direction	0.61	1.86

Figure 7 depicts FFT analysis of CT waveforms of reference design and upgraded design. The fundamental, 2nd order and 3rd order components of CT are significantly reduced on the application of the slot opening shift approach.

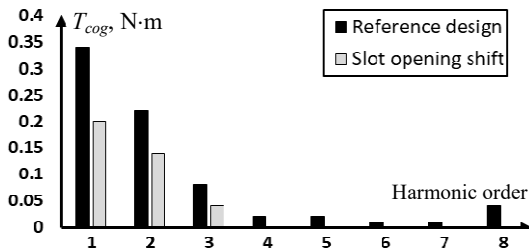


Fig. 7. Comparison of FFT analysis of CT

Figure 8 shows a comparison of the reference design's average torque and that of an upgraded design employing the slot opening shift method. The reference design produces an average torque of 1.91 N-m. When the slot opening of all slots is shifted in an anticlockwise direction, the average torque attained is 1.86 N-m. Thus, using the slot opening modification approach, the CT of the surface PM motor is substantially reduced while average torque is marginally reduced.

Figure 9 shows back EMF profiles for reference and upgraded designs. The amplitude of the back EMF waveform is marginally lowered in the modified design compared to the reference design.

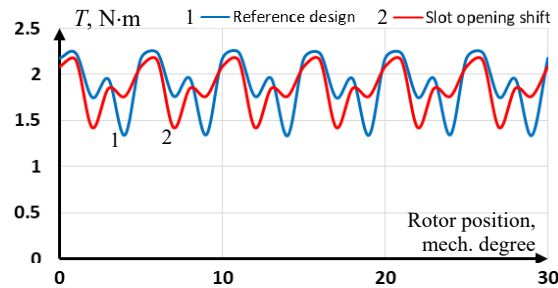


Fig. 8. Comparison of torque profiles of reference design and upgraded design

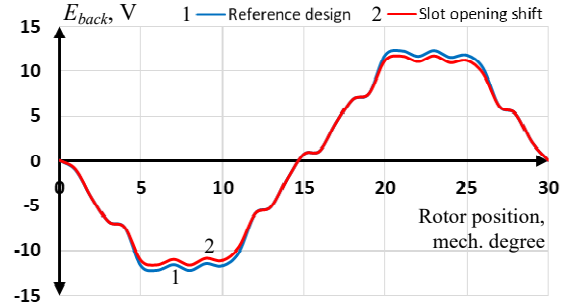


Fig. 9. Comparison of back EMF profile of reference design and upgraded design

Figure 10 shows the back EMF's harmonic spectrum for both the reference and upgraded designs. The total harmonic distortion (THD) of the reference design is 8.03 % while the THD of the upgraded design is 6.9 %. Hence, it is analyzed that the quality of back EMF waveform is improved with a reduction in THD.

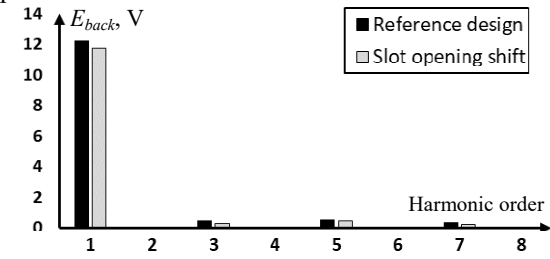


Fig. 10. Comparison of FFT analysis of back EMF

Flux densities are assessed in different motor sections using electromagnetic field analysis. This helps to demonstrate the correctness of improved and reference designs. Figures 11, 12 show the flux density distributions for the reference design and the upgraded designs.

Conclusions. This research presents a slot opening shift technique to reduce the CT of a surface PMBLDC motor.

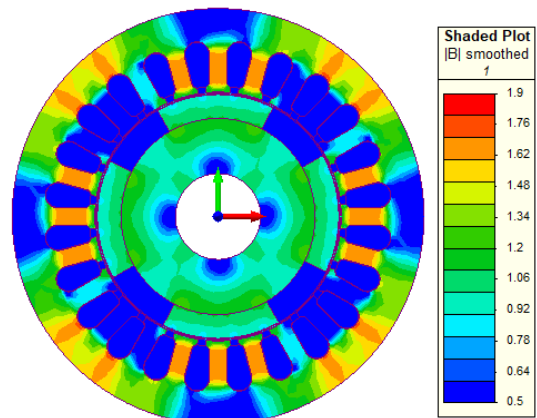


Fig. 11. Distribution of flux density in the reference design

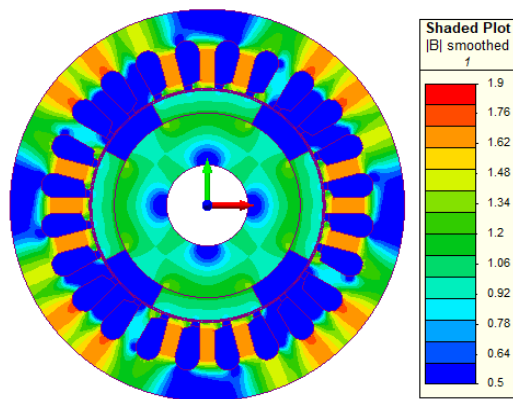


Fig. 12. Distribution of flux density in upgraded design having slot-opening shifted anticlockwise

The reference design for a 200 W, 1000 rpm surface-mounted BLDC motor does not include any shifting of slot opening. The design is upgraded with the slot opening of all slots shifted in an anticlockwise direction by 3.75° mechanical keeping the center line of slots unchanged. The CT waveform of reference and upgraded designs is obtained from FE modelling and analysis. It is observed that with the application of the slot opening shift approach peak-to-peak CT of the surface PMSM motor is reduced by 44.5 % with a borderline reduction in average torque. The slot opening shift approach is a practically implementable approach without any extra manufacturing difficulty and cost. The slot opening shift is an effective and practical method for reducing the CT of a surface PMSM motor.

Conflict of interest. The authors declare that they have no conflicts of interest.

REFERENCES

- Hanselman D.C. *Brushless Permanent Magnet Motor Design*. Magna Physics Publ., Ohio, 2006. 411 p.
- Hendershot J.R., Miller T.J.E. *Design of Brushless Permanent Magnet Motors*. Oxford, Magna Physics & Clarendon Press, 1995. 580 p.
- Chen Y., Fang Z., Chen K., Luo J., Pan J.F. Design and Co-Simulation of High-Speed Permanent Magnet Brushless DC Motor. *2022 IEEE 9th International Conference on Power Electronics Systems and Applications (PESA)*, 2022, pp. 1-4. doi: <https://doi.org/10.1109/PESA55501.2022.10038434>.
- Diao C., Zhao W., Wang N., Wang X. Analysis of a High-Speed Axial Flux Permanent Magnet Motor With Hybrid Magnets for Low Cost. *2022 IEEE 20th Biennial Conference on Electromagnetic Field Computation (CEFC)*, 2022, pp. 1-2. doi: <https://doi.org/10.1109/CEFC55061.2022.9940827>.
- Panchal T.H., Patel A.N., Patel R.M. Reduction of cogging torque of radial flux permanent magnet brushless DC motor by magnet shifting technique. *Electrical Engineering & Electromechanics*, 2022, no. 3, pp. 15-20. doi: <https://doi.org/10.20998/2074-272X.2022.3.03>.
- Patel A.N., Doshi P.J., Mahagoakar S.C., Panchal T.H. Optimization of cogging torque in interior permanent magnet synchronous motor using optimum magnet v-angle. *Electrical Engineering & Electromechanics*, 2023, no. 6, pp. 16-20. doi: <https://doi.org/10.20998/2074-272X.2023.6.03>.
- Athira R.S., Binu L.S. Techniques for Torque Ripple Reduction in BLDC Motor for EV. *2023 International Conference on Circuit Power and Computing Technologies (ICCPCT)*, 2023, pp. 1008-1014. doi: <https://doi.org/10.1109/ICCPCT58313.2023.10245720>.
- Tsunata R., Takemoto M. Skewing Technology for Permanent Magnet Synchronous Motors: A Comprehensive Review and Recent Trends. *IEEE Open Journal of the Industrial Electronics Society*, 2024, vol. 5, pp. 1251-1273. doi: <https://doi.org/10.1109/OJIES.2024.3491295>.
- Hua T., Wang A., Jiang Y., Gu L. Study on the Weakening of Cogging Torque by Stator Structure Optimization of Permanent Magnet Synchronous Motor. *2024 IEEE International Conference on Electrical Energy Conversion Systems and Control (IEECSC)*, 2024, pp. 53-57. doi: <https://doi.org/10.1109/IEECSC62814.2024.10913732>.
- Kim K., Hwang M., Cha H. Cogging Reduction Method for Axial Flux Permanent Magnet Motor Utilizing Skew-Shaped Slot Rotor. *2024 IEEE 6th Eurasia Conference on Biomedical Engineering, Healthcare and Sustainability (ECBIOS)*, 2024, pp. 504-509. doi: <https://doi.org/10.1109/ECBIOS61468.2024.10885473>.
- Lee S.-W., Yang I.-J., Kim W.-H. A Study on Reducing Cogging Torque of IPMSM Applying Rotating Tapering. *IEEE Transactions on Magnetics*, 2022, vol. 58, no. 8, pp. 1-5. doi: <https://doi.org/10.1109/TMAG.2022.3179126>.
- Dai L., Niu S., Gao J., Liu K., Huang S., Chan W.L. Diverse Slot-Opening Designs for Cogging Torque and Performance Optimization in PM Machines. *IEEE Transactions on Transportation Electrification*, 2025, vol. 11, no. 3, pp. 8414-8426. doi: <https://doi.org/10.1109/TTE.2025.3540837>.
- Banchhor D.K., Jain A.K., Dalal A. Effect of Eccentric Tooth Tip Arc on Cogging Torque of PM Machines. *2023 IEEE 2nd Industrial Electronics Society Annual On-Line Conference (ONCON)*, 2023, pp. 1-6. doi: <https://doi.org/10.1109/ONCON60463.2023.10431049>.
- Kobayashi M., Morimoto S., Sanada M., Inoue Y. A Novel Design for Notch on Rotor Surface of Double-Layered Interior Permanent Magnet Synchronous Motor for Reducing Cogging Torque. *2020 International Conference on Electrical Machines (ICEM)*, 2020, pp. 39-44. doi: <https://doi.org/10.1109/ICEM49940.2020.9270972>.
- Imanuddin N., Furqani J., Rizqiawan A. Effects of Radial Divided Magnet Shifting on Cogging Torque of Axial Flux Permanent Magnet Generator for Small Scale Wind Turbine. *2023 4th International Conference on High Voltage Engineering and Power Systems (ICHVEPS)*, 2023, pp. 555-560. doi: <https://doi.org/10.1109/ICHVEPS58902.2023.10257501>.
- Wan X., Yang S., Li Y., Shi Y., Lou J. Minimization of Cogging Torque for V-Type IPMSM by the Asymmetric Auxiliary Slots on the Rotor. *IEEE Access*, 2022, vol. 10, pp. 89428-89436. doi: <https://doi.org/10.1109/ACCESS.2022.3201246>.
- Wang B., Wang D., Peng C., Wang C., Xu C., Wang X. Interior Permanent Magnet Synchronous Machines With Composed T-Shaped Notching Rotor. *IEEE Transactions on Industrial Electronics*, 2024, vol. 71, no. 6, pp. 5519-5529. doi: <https://doi.org/10.1109/TIE.2023.3292854>.
- Yuan B., Li H., Xiang X., Zhou T., Zhou H., Jiang P. Investigation of Cogging Torque Comprehensive Reduction Method in High Precision Servo Permanent Magnet Motor. *2022 25th International Conference on Electrical Machines and Systems (ICEMS)*, 2022, pp. 1-4. doi: <https://doi.org/10.1109/ICEMS56177.2022.9983382>.
- Ding J., Jiang W. Effect of Stator Auxiliary Groove on the Vibration and Noise of Permanent Magnet Synchronous Motor. *2024 IEEE International Conference on Electrical Energy Conversion Systems and Control (IEECSC)*, 2024, pp. 32-36. doi: <https://doi.org/10.1109/IEECSC62814.2024.10913734>.
- Zon B., Wegiel T. Analysis of Cogging Torque Reduction Method Effectiveness on the Example of a Surface Mounted Permanent Magnet Synchronous Motor Model. *2018 International Symposium on Electrical Machines (SME)*, 2018, pp. 1-5. doi: <https://doi.org/10.1109/ISEM.2018.8442778>.
- Ocak O., Aydin M. An Innovative Semi-FEA Based, Variable Magnet-Step-Skew to Minimize Cogging Torque and Torque Pulsations in Permanent Magnet Synchronous Motors. *IEEE Access*, 2020, vol. 8, pp. 210775-210783. doi: <https://doi.org/10.1109/ACCESS.2020.3038340>.
- Grechko O.M. Influence of the poles shape of DC electromagnetic actuator on its thrust characteristic. *Technical Electrodynamics*, 2024, no. 1, pp. 38-45. doi: <https://doi.org/10.15407/techned2024.01.038>.
- Liu T., Huang S., Gao J., Lu K. Cogging Torque Reduction by Slot-Opening Shift for Permanent Magnet Machines. *IEEE Transactions on Magnetics*, 2013, vol. 49, no. 7, pp. 4028-4031. doi: <https://doi.org/10.1109/TMAG.2013.2239977>.

Received 11.08.2025

Accepted 23.11.2025

Published 02.03.2026

A.N. Patel¹, PhD, Associate Professor,

T.H. Panchal¹, PhD, Assistant Professor,

¹ Department of Electrical Engineering, Institute of Technology,

Nirma University, Ahmedabad, Gujarat, India,

e-mail: amit.patel@nirmauni.ac.in;

tejas.panchal@nirmauni.ac.in (Corresponding Author)

How to cite this article:

Patel A.N., Panchal T.H. Mitigation of cogging torque in surface permanent magnet brushless DC motor using slot opening shift. *Electrical Engineering & Electromechanics*, 2026, no. 2, pp. 10-14. doi: <https://doi.org/10.20998/2074-272X.2026.2.02>